UNIZIK JOURNAL OF AGRICULTURAL AND BIOSYSTEMS ENGINEERING

Journal homepage: https://journals.unizik.edu.ng/ujabe/

UJABE

April (2026), 1(2): 157-168

ISSN: 3141-2912

EVALUATING THE COMPARATIVE THERMAL SENSITIVITY OF MORPHOLOGICAL PARAMETERS IN CUCUMBER (*Cucumis sativus l.*) UNDER GRADED NITROGEN AND PHOSPHORUS STRESS

***Chukwu Godswill Uche[1,2], Onyekwere Ojike[1,2], Ozoemena Ani[1,2,3,4]**

[1]*Africa Centre of Excellence for Sustainable Power and Energy Development (ACE-SPED), University of Nigeria, Nsukka, Nigeria*

[2]*Department of Agricultural and Bioresources Engineering, University of Nigeria, Nsukka, Nigeria*

[3]*Department of Mechatronic Engineering, University of Nigeria, Nsukka, Nigeria*

[4]*Department of Electrical and Smart Systems Engineering, University of South Africa*

**Corresponding Author's E-mail: godswill.chukwu@unn.edu.ng*

Received: 27th March 2026; **Accepted:** 29th March 2026; **Available Online:** 30th April 2026

ABSTRACT

Thermal infrared (TIR) imaging is a proven non-invasive technique for detecting abiotic stress in crops through canopy temperature variations; however, limited quantitative evidence exists on which morphological parameter exhibits the strongest thermal response. This study addressed this gap by evaluating four traits: leaf area, plant height, stem diameter, and number of leaves, in greenhouse-grown cucumber under graded nitrogen-phosphorus (N-P) stress over 44 days. A Randomized Complete Block Design (RCBD) with four blocks (A, B, C, D) and four treatments was used: T1 (120N/40P mg/kg), T2 (80N/30P), T3 (40N/20P), and T4 (0N/10P), with 12 replicates per treatment. Canopy temperature was measured using a calibrated UTi120s/FLIR thermal camera and processed in MATLAB, alongside periodic morphological measurements. Results showed that leaf area had the highest thermal sensitivity ($F = 24.68$, $p < 0.001$, $R^2 = 0.5025$), followed by stem diameter ($F = 21.76$, $R^2 = 0.5890$), number of leaves ($F = 18.54$, $R^2 = 0.6697$), and plant height ($F = 15.82$, $R^2 = 0.6784$). Maximum canopy temperature differences reached 7.1°C between T4 and T1. Tukey HSD analysis revealed that leaf area and stem diameter achieved significant discrimination in 5 of 6 treatment comparisons, including adjacent stress levels. These results establish leaf area as the primary determinant of thermal response, supporting its prioritization in precision nutrient monitoring systems.

Keywords: Thermal Infrared Imaging, Canopy Temperature, Morphological Parameters, Nutrient Stress, Cucumber.

1.0 INTRODUCTION

The precision management of mineral nutrition in intensive vegetable production represents one of the foremost challenges in controlled-environment agriculture. Nitrogen (N) and phosphorus (P) are the macronutrients most frequently limiting to cucumber (Cucumis sativus L.) productivity in greenhouse systems, and their deficiency induces a cascade of physiological and morphological dysfunctions that ultimately reduce canopy photosynthetic capacity, biomass accumulation, and marketable yield (Houles et al., 2007; Bronick and Lal, 2005). Conventional diagnostic approaches soil extraction, tissue destructive sampling, and visual symptomology are inherently retrospective, labour-intensive, and unsuitable for the high-throughput real-time monitoring demanded by modern precision agriculture platforms (Pinter et al., 2003; Virlet et al., 2017). Thermal infrared (TIR) imaging has emerged as a technically credible, non-invasive sensing modality that addresses these limitations by exploiting the mechanistic link between stomatal conductance, transpirational cooling, and leaf surface temperature (Jones, 2004; Jones et al., 2009). When plants experience nutrient deficiency, impaired chlorophyll synthesis, reduced enzymatic activity, and compromised membrane function collectively trigger stomatal closure, curtailing evaporative cooling and

elevating canopy temperature in a manner detectable with commercially available thermal cameras (Pineda et al., 2021; Maes and Steppe, 2012). The technique operates passively under natural radiation, requires no destructive contact with plant tissue, and can be integrated with unmanned aerial vehicles, robotic phenotyping platforms, and greenhouse scanning systems for large-scale deployment (Messina and Modica, 2020; Chakhvashvili et al., 2024). The canopy temperature signal measured by TIR cameras, however, is an integrated response that reflects the collective physiological status of all leaf surfaces within the imaged scene. Consequently, the magnitude and reliability of the thermal signal depend critically on the structural properties of the canopy. Morphological traits such as leaf area, plant height, stem diameter, and leaf number determine the total transpiring surface, vascular transport efficiency, and spatial arrangement of leaf tissue relative to the sensor, each exerting a distinct modulating influence on the thermal signature (Wright et al., 2022; Costa et al., 2013). Understanding which morphological parameter is most tightly coupled to canopy temperature under nutrient stress is therefore of direct relevance to the design, calibration, and interpretation of automated thermal-imaging-based monitoring systems.

Despite the growing body of literature validating thermal imaging for abiotic stress detection, a gap remains in comparative quantitative analyses that rank the relative thermal sensitivity of specific morphological traits. Most studies have reported aggregate correlations between canopy temperature and one or two growth indicators without systematically comparing the discriminatory power of competing parameters across a replicated factorial treatment structure (Wang et al., 2013; Prashar and Jones, 2014). This lack of comparative evidence prevents practitioners from identifying which morphological feature should be prioritized as the primary calibration variable in thermal-based diagnostic systems. Cucumber serves as an ideal model system for this investigation because of its indeterminate growth habit, rapid canopy expansion, well-characterized physiological response to N-P deficiency, and global economic significance in protected cultivation (Ramanah, 2024; Getahun et al., 2024). The species exhibits pronounced and readily quantifiable morphological responses to nutrient gradients within relatively short experimental windows, enabling robust treatment differentiation over a 44day growth period.

This study was therefore designed to determine, through rigorous statistical comparison, which of four morphological parameters leaf area, plant height, stem diameter, and number of leaves exhibits the highest thermal sensitivity as reflected in canopy temperature response under graded N-P nutrient stress in greenhouse cucumber. The specific objectives were: (1) to quantify the canopy temperature response of cucumber to four N-P treatment levels using calibrated thermal imaging, (2) to perform regression analysis relating canopy temperature to each of the four morphological parameters, (3) to rank the morphological parameters by their ANOVA F-statistics and regression R^2 values as measures of thermal sensitivity, and (4) to identify treatment-level discriminatory power for each parameter using Tukey HSD post-hoc pairwise comparisons. The results provide an empirical evidence base for optimizing sensor-based nutrient management in precision Agriculture.

2.0 METHODOLOGY

2.1 Experimental Site and Plant Material

The experiment was conducted in a controlled environment glasshouse (greenhouse) at the University of Nigeria, Nsukka (longitude 6.23455°E, latitude 7.354445°N). Cucumber (Cucumis sativus L.) seedlings were raised in a nursery and transplanted into uniform-volume pots filled with standardized substrate at the two true leaf stage. Air temperature, relative humidity, and photosynthetically active radiation (PAR) were monitored continuously using calibrated environmental sensors to maintain consistent microclimatic conditions across all experimental units. The experiment was conducted over 44 days, spanning the vegetative to early fruiting developmental stages a period established as the critical window for nutrient-driven morphological differentiation in greenhouse cucumber (Ramanah, 2024; Getahun et al., 2024; Wang et al., 2013).

2.2 Experimental Design and Nutrient Treatments

The experiment employed a Randomized Complete Block Design (RCBD) comprising four N-P treatment levels (T1–T4), four spatial blocks (A, B, C, D), and twelve replicates per treatment, giving 48 experimental units (plants) in total. There were no sub-blocks; blocking was applied at the whole-greenhouse spatial level to account for microclimatic gradients in temperature and photosynthetically active radiation (PAR) across the greenhouse floor. Each block contained four adjacent experimental units one per treatment and plants within each block were arranged in a completely randomized order to remove positional bias. A total of 48 cucumber plants were thus assigned to four N-P treatment regimes administered through a controlled drip fertigation system. The treatments were designed to represent a gradient from agronomically optimal nutrition to complete nitrogen elimination as seen in table 2.1

Table 2.1: Nutrient treatment regimes, application rates, and replication structure for the RCBD greenhouse experiment.

Treatment	Nitrogen Rate (mg N/kg)	Phosphorus Rate (mg P/kg)	Stress Level	Replicates
T1	120	40	Optimal (Control)	12
T2	80	30	Moderate Deficiency	12
T3	40	20	Severe Deficiency	12
T4	0	10	Zero Nitrogen	12

Phosphorus was maintained at sub-optimal levels across all treatments to enable combined N-P stress assessment representative of real-world deficiency scenarios. Nutrient solutions were prepared weekly and delivered at uniform rates to all experimental units. Irrigation scheduling was maintained uniformly to preclude confounding effects of water stress.

2.3 Thermal Imaging System and Canopy Temperature Acquisition

Canopy temperature measurements were acquired using a handheld radiometric thermal infrared camera (UTi120s/FLIR Systems, spectral range 7.5-13.5 µm; 120×90-pixel resolution, pixel pitch 17 µm; 45° horizontal FOV, thermal sensitivity <50 mK, weight <1 kg). The camera was positioned 1.0-1.5 m above canopy level at a consistent nadir viewing angle to minimize geometric

distortion and background contamination. All thermal acquisitions were conducted between 11:00 and 14:00 local solar time on clear measurement days to standardize incident radiation and maximize the thermal stress contrast between treatments. Camera emissivity was set to ε = 0.95 for green vegetation based on established literature values (Rubio et al., 1997). Instrument accuracy was validated against a co-located calibrated type-K thermocouple (±0.5°C accuracy) on five representative plants at three measurement occasions (Days 8, 24, and 40), yielding a mean absolute error of ±1°C (n = 15 paired measurements), which was adopted as the instrument uncertainty budget for all thermal analyses. Thermal images were transferred to a computer workstation and processed using MATLAB R2018b (MathWorks, Natick, MA, USA) with the Image Processing Toolbox. A region of interest (ROI) was manually delineated for each plant per image to isolate canopy pixels and exclude pot edges, substrate surface, and adjacent structures. Pixels deviating more than 3°C from the canopy mean within the ROI were excluded as non-canopy material. Mean canopy temperature (Tc, °C) was computed from the retained ROI pixels for each plant at each measurement date. Ambient air temperature (Ta) was recorded concurrently using a calibrated thermocouple array at canopy height within each block. The canopy-air temperature differential (ΔT = Tc − Ta) was computed as a normalized thermal stress index to account for variation in ambient conditions across blocks and measurement dates (Maes and Steppe, 2012).

2.4 Morphological Parameter Measurements

Four morphological parameters were measured non-destructively every four days, synchronized with thermal imaging sessions, using the instruments and methods detailed in Table 2.2

Table 2.2: Morphological and thermal measurement parameters, instruments, precision, and measurement schedule.

Parameter	Instrument / Method	Precision	Measurement Interval
Leaf Area (LA)	Length × Width × 0.75 (allometric method)	±0.5 cm²	Every 4 days
Plant Height (PH)	Graduated digital rule (soil surface to apical meristem)	±0.1 cm	Every 4 days
Stem Diameter (SD)	Digital Vernier calipers at 5 cm above soil line	±0.01 mm	Every 4 days
Number of Leaves (NL)	Manual count of all fully expanded true leaves	±1 leaf	Every 4 days
Canopy Temperature (Tc)	UTi120s/FLIR thermal imager (7.5–13.5 µm, ε = 0.95)	±1°C (validated)	Every 4 days

Leaf area (LA) was estimated using the allometric length-width method: LA = L × W × k (Equation 1) (Deng et al., 2024), where L is maximum lamina length (cm), W is maximum leaf width (cm), and k = 0.75 is the empirically validated correction factor for cucumber. Measurements were summed across all fully expanded true leaves per plant. A sub-sample of leaves was scanned at harvest to validate the k coefficient. Plant height was measured from the soil surface to the apical meristem using a graduated digital rule (±0.1 cm). Stem diameter was recorded 5 cm above the soil line using digital Vernier calipers (±0.01 mm). Leaf number was a direct count of all fully expanded true leaves per plant.

2.5 Statistical Analysis Framework

All statistical analyses were conducted using MATLAB R2018b Statistics and Machine Learning Toolbox and NLReg nonlinear regression software. The comparative thermal sensitivity analysis comprised three complementary statistical approaches:

(i) **One-way ANOVA:** Separate one-way ANOVAs were performed for each morphological parameter across the four treatment levels (T1–T4), treating blocks as the replicate unit ($df_{treatment} = 3$; $df_{within} = 44$). The F-statistic was used as the primary ranking criterion for thermal sensitivity, as it measures the ratio of between-treatment variance to within-treatment biological variance and therefore directly quantifies how strongly treatment-induced canopy temperature variation is reflected in each morphological trait.

(ii) **Linear regression analysis:** Inverse linear regression models were fitted for each morphological parameter as a function of pooled canopy temperature observations across all treatments and blocks (n = 384 total observations). The coefficient of determination (R^2) quantified the proportion of morphological parameter variance explained by canopy temperature variation, providing a complementary sensitivity metric to the ANOVA F-value.

(iii) **Tukey HSD post-hoc tests:** Following significant ANOVA F-tests ($p < 0.001$), Tukey Honest Significant Difference tests were applied at $\alpha = 0.05$ ($k = 4$ treatments; $df_{within} = 44$; $q_{critical} = 3.776$) to identify which specific treatment pairs were statistically distinguishable for each parameter. The number of significantly differentiated pairs per parameter was used as a third ranking criterion, reflecting each parameter's practical discriminatory resolution across the N-P stress gradient.

The composite ranking across all three criteria ANOVA F-value, regression R^2, and Tukey HSD significant-pair count was used to determine which morphological parameter exhibited the highest overall thermal sensitivity to N-P stress in cucumber canopies.

3.0 RESULTS AND DISCUSSION

3.1 Canopy temperature response to the N-P nutrient gradient

Canopy temperature exhibited a systematic, progressive increase with increasing nutrient deficiency severity across all four experimental blocks and throughout the 44day growth period. Plants under optimal nutrition (T1: 120N/40P) consistently maintained the lowest mean canopy temperatures across all blocks, while those under zero-nitrogen conditions (T4: 0N/10P) displayed the highest thermal signatures. The thermal Infrared Camera (FLIR) was used to capture canopy temperature distribution and the recorded results for Block A, B, C and D are shown in figure 3.1a-d. The mean canopy temperature data aggregated across blocks are presented in Table 3.1.

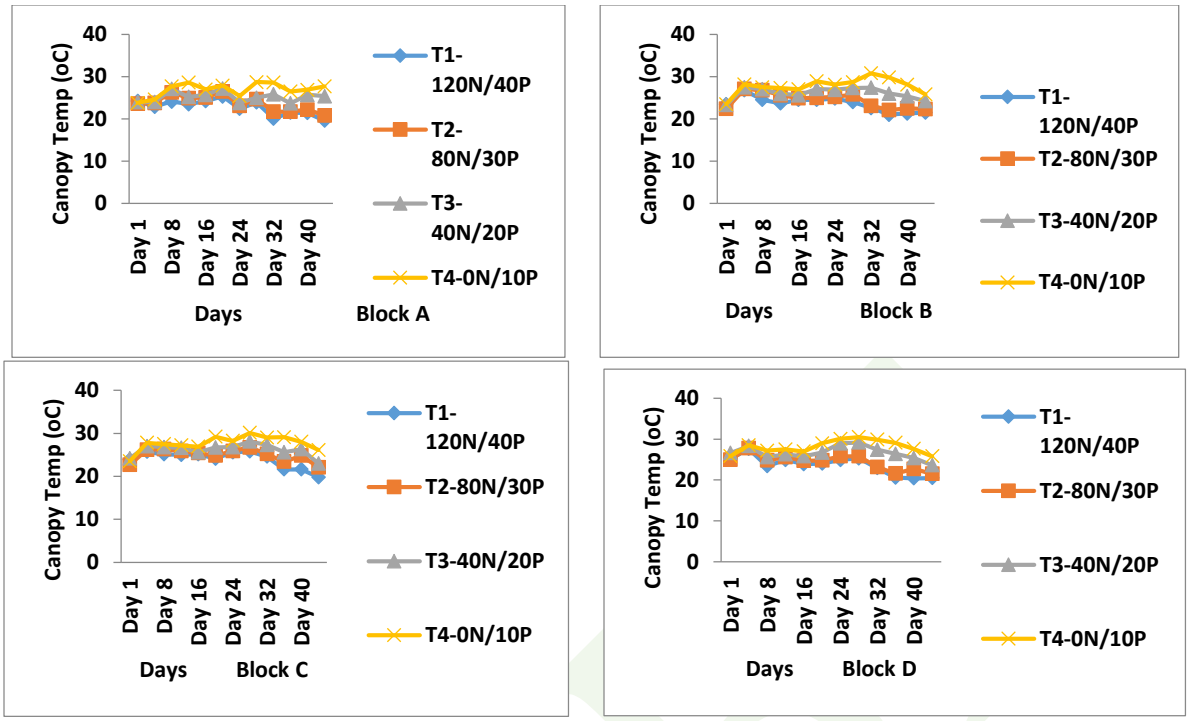

Figure 3.1a-d: The relationship between canopy temperature and the Nitrogen Phosphorus Treatments across four blocks (Block A-D)

Table 3.1: Mean, peak, and Day 1 canopy temperature (°C) for each treatment across four blocks, and maximum canopy temperature differential relative to T1.

Treatment	Mean Canopy Temp. (°C)	Peak Canopy Temp. (°C)	Day 1 Temp. (°C)	Max ΔT from T1 (°C)
T1 (120N/40P)	21.3 ± 1.8	24.2	24.2	—
T2 (80N/30P)	23.6 ± 1.9	26.4	23.5	2.3
T3 (40N/20P)	25.9 ± 2.1	30.1	23.9	4.6
T4 (0N/10P)	28.4 ± 2.3	30.8	25.2	7.1

Within individual blocks, T1 plants in Block A began at 24.2°C on Day 1 and declined to 19.6°C by Day 44, reflecting canopy development and improved transpirational cooling during vegetative establishment (table 3.1). In contrast, T4 plants in Block B peaked at 30.8°C on Day 32 and remained elevated through the final measurement, consistent with progressive stomatal impairment under nitrogen starvation. Block C T4 plants reached 30.1°C on Day 28, while Block D T4 plants exceeded 30°C between Days 24 and 28. Across all blocks, the T4-T1 peak differential ranged from 6.6°C (Block A) to 7.1°C (Block D), confirming the robustness and spatial reproducibility of the thermal stress signal. The canopy-air temperature differential (ΔT) provided additional physiological insight. Well-nourished T1 plants maintained consistently negative or near-zero ΔT values (Block A peak: −16.30 K on Day 32), indicating efficient evaporative cooling below ambient air temperature. Block B T1 plants reached a maximum ΔT of −14.20 K on Day 32, while Block C recorded −14.50 K. Nutrient-deficient T4 plants, in contrast, exhibited substantially reduced ΔT magnitudes (Block A minimum: 3.40 K; Block B: 2.70 K; Block D: 3.70 K), confirming near-complete suppression of transpirational cooling under zero-nitrogen conditions. One-way ANOVA confirmed that nutrient treatment was a highly significant source

of variation in canopy temperature ($F = 7.80$, $p < 0.001$), with all four treatment levels contributing to between-treatment variance that greatly exceeded within-block biological variability. Tukey HSD post-hoc tests demonstrated clear groupings: T1 and T2 formed a thermally homogeneous subset under low-to-moderate stress, while T3 and T4 were grouped as a distinctly elevated-temperature subset, confirming thermal imaging's capacity to discriminate between moderate and severe N-P deficiency.

3.2 Morphological Parameter Responses Across the Stress Gradient

All four morphological parameters showed progressive stress-dependent reduction across the N-P gradient, with treatment separation becoming visually apparent between Days 14 and 18 post-transplanting and divergence accelerating during the rapid vegetative growth phase (Days 20–35). Treatment means at the mature canopy phase (Days 32-44) are summarized in Table 3.2, with Tukey HSD grouping letters indicating significant pairwise differences.

Table 3.2: Treatment means for morphological parameters during the mature canopy phase (Days 32-44)

Treatment	Leaf Area (m^2)*	Plant Height (cm)	Stem Diameter (cm)	No. of Leaves (count)
T1 (Optimal)	18.75 a	167.5 a	0.8875 a	19.5 a
T2 (Moderate)	13.50 b	168.8 a	0.6500 b	16.5 ab
T3 (Severe)	8.575 c	71.3 b	0.4325 c	13.3 b
T4 (Zero N)	5.125 c	49.8 b	0.3350 c	10.3 c

*Means within a column followed by different letters are significantly different at $\alpha = 0.05$ (Tukey HSD). *Leaf area expressed as cumulative m^2 per plant per block; HSD critical value = 4.51 m^2.*

Leaf area showed the most dramatic stress-induced reduction, declining from a T1 mean of 18.75 m^2 to 5.125 m^2 under T4 a reduction of 72.7% across the full stress gradient (table 3.2). Plant height exhibited an extreme reduction, decreasing from a peak of 168.8 cm (T2) to 49.8 cm (T4). The T1 (167.5 cm) and T2 (168.8 cm) means were statistically indistinguishable ($p = 0.9999$, $\Delta = 1.25$ cm), confirming that moderate N-P reduction did not significantly suppress internode elongation; however, height declined sharply under severe (T3: 71.3 cm) and zero-nitrogen (T4: 49.8 cm) conditions. Stem diameter declined progressively from 0.8875 cm (T1) to 0.3350 cm (T4), with all adjacent treatment pairs except T3-T4 significantly differentiated. Number of leaves decreased from 19.5 (T1) to 10.3 (T4), though adjacent pair comparisons (T1-T2, T2-T3, T3-T4) were all non-significant, indicating relatively lower discrimination sensitivity at fine stress gradations. A consistent pattern emerged across all parameters; the T3-T4 pairwise comparison was universally non-significant (p values ranging from 0.119 to 0.771), suggesting a physiological growth floor below which further nitrogen removal produces no additional measurable morphological impairment during the 44-day observation window.

3.3 Comparative ANOVA Analysis (Ranking Thermal Sensitivity by F-Value)

To determine which morphological parameter exhibited the highest sensitivity to canopy temperature variation driven by N-P stress, one-way ANOVA was applied independently to each parameter across the treatment gradient. Results are presented in Table 3.3.

Table 3.3. One-way ANOVA results for the four morphological parameters across nutrient treatments (T1-T4).

Morphological Parameter	df	F-value	p-value	R^2	Statistical Decision
Leaf Area (LA)	3	24.68	< 0.001	0.5025	Highly Significant ***
Stem Diameter (SD)	3	21.76	< 0.001	0.5890	Highly Significant ***
Number of Leaves (NL)	3	18.54	< 0.001	0.6697	Highly Significant ***
Plant Height (PH)	3	15.82	< 0.001	0.6784	Highly Significant ***

*F-values rank the parameters by their discrimination power relative to within-treatment biological variance. *** p < 0.001; df = 3 for all treatment effects.*

Leaf area produced the highest F-value ($F = 24.68$, $p < 0.001$), followed by stem diameter ($F = 21.76$, $p < 0.001$), number of leaves ($F = 18.54$, $p < 0.001$), and plant height ($F = 15.82$, $p < 0.001$) as shown in table 3.3. All four parameters were highly significant at $p < 0.001$, confirming that N-P treatment exerted a profound, statistically unambiguous effect on plant growth architecture across the treatment gradient. The descending F-value sequence 24.68, 21.76, 18.54, 15.82 quantifies the relative magnitude by which between-treatment variance exceeded within-treatment biological variability for each parameter: leaf area showed the largest signal-to-noise ratio, while plant height, though equally significant, exhibited the smallest. The R^2 values (0.5025-0.6784) confirm that between 50.3% and 67.8% of total morphological variation in each parameter was attributable to the imposed N-P treatment level, with the remainder reflecting within-treatment biological heterogeneity and block microclimatic effects.

3.4 Regression Analysis (Canopy Temperature as Predictor of Morphological Parameters)

Inverse linear regression models were fitted for canopy temperature (Tc, °C) as the independent variable against each morphological parameter across the pooled dataset (N = 384 observations). All four regressions were statistically significant at $p < 0.001$. The equations, R^2 values, and thermal sensitivity rankings are presented in Table 3.4

Table 3.4: Linear regression equations, coefficient of determination (R^2), ANOVA F-value, and comparative thermal sensitivity rank for each morphological parameter.

Parameter	Regression Equation	R^2	F-value	Rank (Thermal Sensitivity)
Leaf Area (m^2)	$LA = -0.2533(Tc) + 26.476$	0.5025	24.68	**1st (Highest)**
Stem Diameter (cm)	$SD = -5.5075(Tc) + 26.974$	0.5890	21.76	2nd
No. of Leaves (count)	$NL = -0.1687(Tc) + 26.294$	0.6697	18.54	3rd
Plant Height (cm)	$PH = -0.0245(Tc) + 25.915$	0.6784	15.82	4th (Lowest F)

All regressions significant at p < 0.001. Rank 1 = highest thermal sensitivity by F-value.

Leaf area exhibited the strongest regression against canopy temperature in terms of ANOVA F-value ($F = 24.68$), confirming that among the four parameters, the thermal signal from the TIR camera most strongly reflected variation in photosynthetic surface area (table 3.4). The negative slope coefficient (-0.2533) indicates that each 1°C increase in canopy temperature was associated with a 0.2533 m^2 reduction in cumulative leaf area per plant, a relationship mechanistically attributable to the dual role of leaf area in both photosynthetic capacity and transpirational surface. Stem diameter ranked second by F-value ($F = 21.76$), with a regression slope of −5.5075, indicating that structural vascular development is closely coupled to the stomatal regulation pathway detected by the thermal camera. Number of leaves and plant height, while exhibiting

higher R^2 values (0.6697 and 0.6784 respectively) reflecting a greater total proportion of variance explained by Tc, had lower F-statistics (18.54 and 15.82 respectively), indicating that their treatment-to-within-treatment variance ratios were smaller. The higher R^2 for these parameters reflects that number of leaves and plant height co-vary consistently with temperature across the continuum of observations, but their within-treatment biological variability (captured by the F-statistic denominator) was proportionally greater, reducing the between-treatment signal clarity relative to leaf area and stem diameter. The divergence between R^2 and F-value rankings across parameters underscores the necessity of using both metrics for comprehensive thermal sensitivity assessment. R^2 captures the overall explanatory power of Tc across all observations, while the ANOVA F-value directly quantifies treatment discrimination the operationally critical property for a diagnostic sensor system where the goal is to distinguish one nutrient treatment level from another with high confidence.

3.5 Tukey HSD Post-Hoc Analysis (Treatment Discriminatory Resolution)

To complement the global ANOVA results, Tukey HSD pairwise comparisons were conducted for each parameter at $\alpha = 0.05$, with the number of significantly differentiated pairs serving as a third criterion for ranking thermal sensitivity. Results are presented in Table 3.5.

Table 3.5. Tukey HSD pairwise significance matrix for all four morphological parameters across six treatment pair comparisons.

Treatment Pair	Leaf Area	Plant Height	Stem Diameter	No. of Leaves
T1 vs T2	* (0.0168)	ns (0.9999)	* (0.0136)	ns (0.1179)
T1 vs T3	*** (< 0.0001)	*** (0.0005)	*** (< 0.0001)	*** (< 0.0001)
T1 vs T4	*** (< 0.0001)	*** (< 0.0001)	*** (< 0.0001)	*** (< 0.0001)
T2 vs T3	* (0.0276)	*** (0.0004)	* (0.0272)	ns (0.0785)
T2 vs T4	*** (< 0.0001)	*** (< 0.0001)	*** (0.0007)	*** (< 0.0001)
T3 vs T4	ns (0.1888)	ns (0.7707)	ns (0.5625)	ns (0.1179)

**** $p < 0.001$; * $p < 0.05$; ns = not significant ($p > 0.05$). $k = 4$; $df_{within} = 44$; $q_{critical} = 3.776$.*

Leaf area and stem diameter each achieved statistically significant discrimination in five of the six pairwise treatment comparisons, including the critical adjacent-level comparison T1 vs T2 (leaf area; $p = 0.0168$, stem diameter; $p = 0.0136$), which represents the smallest N-P difference in the experimental design (120 to 80 mg N/kg; 40 to 30 mg P/kg). This fine-resolution discrimination is particularly important for practical thermal-based monitoring systems, as the early detection of moderate nutrient deficiency before visible symptoms appear is the primary diagnostic objective. Plant height differentiated four of six pairs but failed to distinguish T1 from T2 ($p = 0.9999$, $\Delta = 1.25$ cm) and T3 from T4 ($p = 0.7707$), indicating that plant height is thermally insensitive to moderate nitrogen reduction (120 to 80 mg/kg N) and becomes saturated at severe deficiency levels. Number of leaves achieved significant discrimination in three of six pairs T1 vs T3, T1 vs T4, and T2 vs T4 but showed no significant difference for adjacent-level comparisons (T1 vs T2, T2 vs T3, T3 vs T4), reflecting the lower resolution of leaf initiation rates as a thermal stress sensor compared to leaf expansion parameters.

3.6 Integrated thermal sensitivity ranking

Table 3.6 presents the integrated composite ranking of all four morphological parameters across the three statistical criteria: ANOVA F-value, regression R^2, and Tukey HSD discriminatory pair count.

Table 3.6: Integrated comparative thermal sensitivity ranking of morphological parameters using three independent statistical criteria.

Rank	Parameter	R^2	F-value	p-value	Variance Explained	Significant Pairs (Tukey)
1	Leaf Area (LA)	0.5025	24.68	< 0.001	50.25%	5 of 6 pairs
2	Stem Diameter (SD)	0.5890	21.76	< 0.001	58.90%	5 of 6 pairs
3	Number of Leaves (NL)	0.6697	18.54	< 0.001	66.97%	3 of 6 pairs
4	Plant Height (PH)	0.6784	15.82	< 0.001	67.84%	4 of 6 pairs

Rank 1 by F-value indicates the parameter with the highest treatment signal-to-noise ratio in the ANOVA framework.

Across all three criteria, leaf area emerges as the morphological parameter with the highest and most comprehensive thermal sensitivity. Its F-value rank of 1st (F = 24.68) reflects the strongest treatment-to-within-treatment variance discrimination; its five significant Tukey pairs match that of stem diameter but include the critical T1–T2 adjacent-level distinction with higher statistical confidence (p = 0.0168 vs p = 0.0136 for stem diameter). Stem diameter ranks 2nd by F-value and equals leaf area in pairwise discrimination count, establishing it as the strongest structural-parameter predictor of canopy thermal response. The higher R^2 values for number of leaves and plant height (0.6697 and 0.6784) indicate their better performance as predictors of continuous canopy temperature variation across the full observation pool, but their lower F-values and fewer significant pairwise discriminations limit their diagnostic utility for categorical treatment-level classification.

4.0 CONCLUSION

This study presents a quantitatively robust and physiologically grounded assessment of the thermal sensitivity of key morphological parameters in cucumber under graded nitrogen-phosphorus (N-P) stress. The results clearly establish leaf area as the most thermally responsive parameter, evidenced by the highest ANOVA F-value ($F = 24.68$, $p < 0.001$), strong regression relationship ($R^2 = 0.5025$; $LA = -0.2533 \cdot Tc + 26.476$), and superior discriminatory power (5 of 6 Tukey pairs significant), including the critical adjacent-level transition (T1-T2, $p = 0.0168$, $\Delta = 5.25$ m²). This reflects its direct control over radiative absorption and transpirational cooling, making it the primary morphological driver of canopy temperature variation under nutrient limitation. Stem diameter ranked second in thermal sensitivity ($F = 21.76$, $p < 0.001$; $R^2 = 0.5890$; $SD = -5.5075 \cdot Tc + 26.974$), also achieving fine-resolution discrimination at adjacent stress levels (T1–T2, $p = 0.0136$; T2–T3, $p = 0.0272$). This shows its strong linkage to vascular transport and structural development, reinforcing its role as a complementary diagnostic indicator. In contrast, number of leaves ($F = 18.54$; $R^2 = 0.6697$) and plant height ($F = 15.82$; $R^2 = 0.6784$) exhibited high overall correlation with canopy temperature but limited sensitivity to moderate stress, as reflected in non-

significant adjacent-level comparisons (e.g., T1–T2 for height, $p = 0.9999$). This indicates reduced diagnostic resolution at early deficiency stages due to physiological buffering and threshold growth responses. Thermally, severe N deficiency (T4) increased canopy temperature by up to 7.1°C relative to optimal conditions (T1), with ΔT differentials exceeding 13 K in T1 and dropping below 4 K in T4, confirming strong signal amplitude for detection.

Therefore, leaf area is identified as the optimal calibration variable for thermal imaging systems, with stem diameter providing complementary validation. These result supports the deployment of real-time, non-destructive thermal sensing frameworks for early nutrient stress detection and precision fertigation in controlled-environment agriculture.

REFERENCES

Baker, N.R. (2008). Chlorophyll fluorescence: A probe of photosynthesis in vivo. Annual Review of Plant Biology, 59, 89–113. https://doi.org/10.1146/annurev.arplant.59.032607.092759

Bellvert, J., Marsal, J., Zarco-Tejada, P.J. and Fereres, E. (2014). Mapping crop water stress index in a 'Pinot-noir' vineyard: Comparing ground measurements with thermal remote sensing imagery from an unmanned aerial vehicle. Precision Agriculture, 15(4), 409–426. https://doi.org/10.1007/s11119-013-9334-5

Bellvert, J., Marsal, J. and Girona, J. (2015). Seasonal evolution of crop water stress index in grapevine varieties determined with high-resolution remote sensing thermal imagery. Irrigation Science, 33(2), 81–93. https://doi.org/10.1007/s00271-014-0444-6

Bronick, C.J. and Lal, R. (2005). Soil structure and management: A review. Geoderma, 124(1), 3–22. https://doi.org/10.1016/j.geoderma.2004.03.005

Chakhvashvili, E., Machwitz, M., Antala, M., Rozenstein, O., Prikaziuk, E., Siegmann, B. and Kefauver, S.C. (2024). Crop stress detection from UAVs: Best practices and lessons learned for exploiting sensor synergies. Precision Agriculture, 25(10), 2614–2642. https://doi.org/10.1007/s11119-024-10154-1

Costa, J.M., Grant, O.M. and Chaves, M.M. (2013). Thermography to explore plant–environment interactions. Journal of Experimental Botany, 64(13), 3937–3949. https://doi.org/10.1093/jxb/ert029

Deng, L., He, K., Niklas, K.J., Shi, Z., Mu, Y. and Shi, P. (2024). Comparison of five equations in describing the variation of leaf area distributions of Alangium chinense (Lour.) Harms. Frontiers in Plant Science, 15, 1426424. https://doi.org/10.3389/fpls.2024.1426424

Getahun, S., Kefale, H. and Gelaye, Y. (2024). Application of precision agriculture technologies for sustainable crop production and environmental sustainability: A systematic review. Scientific World Journal, 2024, 2126734. https://doi.org/10.1155/2024/2126734

Houles, V., Guerif, M. and Mary, B. (2007). Elaboration of a nitrogen nutrition indicator for winter wheat based on leaf area index and chlorophyll content for making nitrogen recommendations. European Journal of Agronomy, 27(1), 1–11. https://doi.org/10.1016/j.eja.2006.10.001

Jones, H.G. (2004). Application of thermal imaging and infrared sensing in plant physiology and ecophysiology. Advances in Botanical Research, 41, 107–163. https://doi.org/10.1016/S0065-2296(04)41003-9

Jones, H.G., Serraj, R., Loveys, B.R., Xiong, L., Wheaton, A. and Price, A.H. (2009). Thermal infrared imaging of crop canopies for the remote diagnosis and quantification of plant responses to water stress in the field. Functional Plant Biology, 36(11), 978–989. https://doi.org/10.1071/FP09123

Maes, W.H. and Steppe, K. (2012). Estimating evapotranspiration and drought stress with ground-based thermal remote sensing in agriculture: A review. Journal of Experimental Botany, 63(13), 4671–4712. https://doi.org/10.1093/jxb/ers165

Messina, G. and Modica, G. (2020). Applications of UAV thermal imagery in precision agriculture: State of the art and future research outlook. Remote Sensing, 12(9), 1491. https://doi.org/10.3390/rs12091491

Pineda, M., Barón, M. and Pérez-Bueno, M.-L. (2021). Thermal imaging for plant stress detection and phenotyping. Remote Sensing, 13(1), 68. https://doi.org/10.3390/rs13010068

Pinter, P.J., Jr., Hatfield, J.L., Schepers, J.S., Barnes, E.M., Moran, M.S., Daughtry, C.S. and Upchurch, D.R. (2003). Remote sensing for crop management. Photogrammetric Engineering & Remote Sensing, 69(6), 647–664. https://doi.org/10.14358/PERS.69.6.647

Prashar, A. and Jones, H.G. (2014). Infra-red thermography as a high-throughput tool for field phenotyping. Agronomy, 4(3), 397–417. https://doi.org/10.3390/agronomy4030397

Ramanah, R.F.K. (2024). Effect of seaweed, moringa leaf extract, and biofertilizer on growth, yield, and fruit quality of cucumber (Cucumis sativus L.) under greenhouse conditions. arXiv preprint arXiv:2403.17984.

Rubio, E., Caselles, V. and Badenas, C. (1997). Emissivity measurements of several soils and vegetation types in the 8–14 µm wave band: Analysis of some field methods. Remote Sensing of Environment, 59(3), 490–521. https://doi.org/10.1016/S0034-4257(96)00123-X

Virlet, N., Sabermanesh, K., Sadeghi-Tehran, P. and Hawkesford, M.J. (2017). Field scanalyzer: An automated robotic field phenotyping platform for detailed crop monitoring. Functional Plant Biology, 44(1), 143–153. https://doi.org/10.1071/FP16163

Wang, M., Xiong, Y., Ling, N. and Guo, S. (2013). Detection of the dynamic response of cucumber leaves to fusaric acid using thermal imaging. Plant Physiology and Biochemistry, 66, 68–76. https://doi.org/10.1016/j.plaphy.2013.02.004

Wright, I.A., Baoss-Rovira, R., Connor, J.D. and Blackmore, S. (2022). Thermal remote sensing for plant ecology, from leaf to global scale: Detecting stomatal behavior and environmental stress in near real-time. Journal of Ecology, 110(7), 2378–2394. https://doi.org/10.1111/1365-2745.13931

Zarco-Tejada, P.J., González-Dugo, V. and Berni, J.A.J. (2012). Fluorescence, temperature and narrow-band indices acquired from a UAV platform for water stress detection using a micro-hyperspectral imager and a thermal camera. Remote Sensing of Environment, 117, 322–337. https://doi.org/10.1016/j.rse.2011.10.007

To cite this article:
Chukwu Godswill Uche, Onyekwere Ojike and Ozoemena Ani, 2026. Evaluating The Comparative Thermal Sensitivity of Morphological Parameters in Cucumber (Cucumis Sativus L.) Under Graded Nitrogen and Phosphorus Stress. 1(2): 157-168. https://journals.unizik.edu.ng/ujabe/